EEET ECOLOGICAL ENGINEERING & ENVIRONMENTAL TECHNOLOGY

Ecological Engineering & Environmental Technology 2022, 23(1), 202–211
https://doi.org/10.12912/27197050/142971
ISSN 2719-7050, License CC-BY 4.0

Received: 2021.07.31
Accepted: 2021.11.10
Published: 2021.12.01

The Efficiency of Mg-Al/Biochar for Methyl Orange and Methyl Red Removal

Arini Fousty Badri[1], Novie Juleanti[2], Risfidian Mohadi[2], Mardiyanto[3], Aldes Lesbani[1,4*]

[1] Graduate School of Mathematics and Natural Sciences, Faculty of Mathematics and Natural Sciences, Universitas Sriwijaya, Jl. Padang Selasa, Bukit Besar, Palembang 30139, Indonesia

[2] Department of Chemistry, Faculty of Mathematics and Natural Sciences, Universitas Sriwijaya, Jl. Palembang-Prabumulih, Km. 32, Ogan Ilir 30662, South Sumatra, Indonesia

[3] Department of Pharmacy, Faculty of Mathematics and Natural Sciences, Universitas Sriwijaya, Jl Palembang-Prabumulih, Km. 32, Ogan Ilir 30662, South Sumatra, Indonesia

[4] Research Center of Inorganic Materials and Complexes FMIPA Universitas Sriwijaya, Jl. Palembang-Prabumulih, Km. 32, Ogan Ilir 30662, South Sumatra, Indonesia

* Corresponding author's e-mail: aldeslesbani@pps.unsri.ac.id

ABSTRACT

MgAl-LDH was directly impregnated with biochar to fabricate MgAl-Biochar (MgAl/BC) and applied to remove methyl orange (MO) and methyl red (MR). The XRD, BET, FTIR, TG-DTA and SEM analyses were conducted to characterize the prepared material. The result of XRD characterization diffraction peaks at 11.47, 22.86, 34.69, and 61.6 shows that the precursor was successfully transformed to MgAl-BC. The FT-IR analysis at vibration 1010, 1381,3447 and 1635 cm^{-1} illustrated that the composite was well formed. The BET analysis showed that the surface area of the MgAl-BC composite was 111.404 m^2/g which was larger than that of the precursor, equal to 23.15 m^2/g. The kinetic model of the adsorption study both MR and MO were fitted to PSO and followed the Langmuir model with adsorption capacities for MR 142.857 mg/g and MO 128.205 mg/g. The regeneration study of composite indicated higher efficiency than the pristine and show good stability of adsorption process in five cycles.

Keywords: MgAl-LDH, MgAl-Biochar, methyl red, methyl orange and regeneration.

INTRODUCTION

Dyes disposal was one of the greatest environment issue which endangers the organisms and human beings (Zhao et al., 2018). Although it causes a lot of negative impacts, dyes are still popular in many industries, such as textile, paper (Juleanti et al., 2021), pharmaceutical and paper industries (Wijaya et al., 2021). Many techniques have been studied in order to eliminate dyes from polluted wastewaters such as coagulation (Demissie et al., 2021), microbial (Duan et al., 2019), activated carbon (Puchana-Rosero et al., 2016; Streit et al., 2019), photocatalysis (Cantarella et al., 2016; Natarajan et al., 2020), and adsorption (Vinsiah et al., 2020). Lately, adsorption became an intriguing technique because of its low cost, ease of work and high efficiency (Bharali & Deka, 2017). Different adsorbents have been researched such as carbon active, graphene (Vinsiah et al., 2020) and layered double hydroxide (LDH) (Oktriyanti et al., 2019).

LDH consists of divalent and trivalent cations which are substituted in the octahedral layer. Diverse kinds of anions, such as carbonate nitrate and chlorin between the two layers which effected the difference in sorption capacities (Lu et al., 2016). LDH is a promising adsorbent which carries balanced cation and negative charge (Santos et al., 2017). The charge balancing gives LDH good cation and anion exchange properties (Tran et al., 2018). There have been many studies applicating LDH as an adsorbent in the adsorption process. Ayawei et al. (2015) used

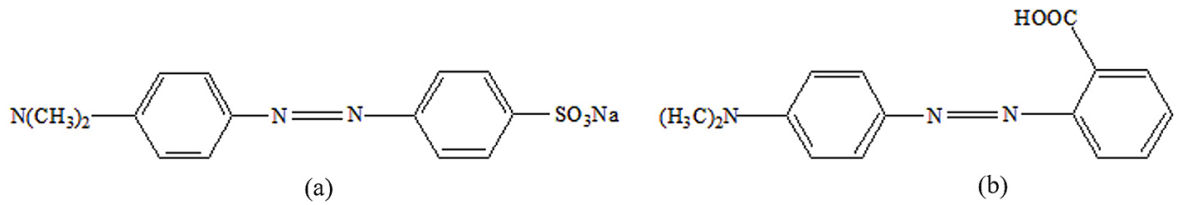

(a) (b)

Figure 1. The chemical structures of MO and MR

MgAl-LDH to remove congo red with adsorption capacity (Q_{max}) of up to 47%. Another study was conducted by synthesizing remove methyl orange with adsorption capacity 205.76 mg/g (Lu et al., 2016). In order to increase the adsorption capacity, LDH can be modified with the other materials such as biochar BC) (Lee et al., 2019). Meili et al. (2019) applied Mg /Al-BC for removing methylene blue with Q_{max} up to 406.47 mg/g. CuAl-BC was fabricated to remove malachite green, reaching equilibrium at 40 minutes with Q_{max} 108.96 mg/L (Palapa et al., 2020).

MgAl LDH was modified with biochar and used for removing organic pollutants which increased the active site of the adsorbent (Gholami et al., 2020). Another research showed Mg-Al-biochar was used to remove phosphate with the co-pyrolysis method (Lee et al., 2019) Thus, MgAl-BC, as an adsorbent, was widely used for reducing organic pollutants. Methyl red (MR) and methyl orange (MO) were categorized as azo dyes with two aromatic rings. The structure of MR and MO was illustrated in Figure 1.

In this research, MgAl-LDH was modified with biochar (BC) to form MgAl-BC for escalating the LDH adsorption capacity. The adsorbents were applied for removing methyl orange (MO) and methyl red (MR). X-ray diffraction, BET, and FT-IR spectra, TG-DTA and SEM analysis were used to characterize the adsorbents. The variation of time, isotherms, and thermodynamics were studied in the adsorption process.

EXPERIMENT

Chemicals and Instrumentations

$Mg(NO_3)_2 \cdot 6H_2O$, $Al(NO_3)_2 \cdot 9H_2O$, Na_2CO_3, NaOH were acquired from Merck and Sigma-Aldrich. XRD was recorded by a Rigaku Miniflex-600. FTIR spectra were obtained by Shimadzu FTIR Prestige-21. BET was calculated using ASAP Quantachrome apparatus. The thermal analysis of materials were studied by TG-DTA Shimadzu and the morphology was measured by SEM Quanta-650 OXFORD.

Synthesis of Mg/Al LDH

Mg/Al LDH was synthesized using coprecipitation method: 0.75 M $Mg(NO_3)_2 \cdot 6H_2O$ as much as 100 mL and 0.25 M $Al(NO_3)_3 \cdot 9H_2O$ as much as 100 mL were mixed and stirred until homogeneous. 50 mL NaOH solution of 2M and 50 mL Na_2CO_3 solution of 2 M were dripped, stirred until homogeneous, then slowly dripped a mixture of $Mg(NO_3)_2 \cdot 6H_2O$ and $Al(NO_3)_3 \cdot 9H_2O$. After being homogeneous, the mixture was maintained for 24 hours at 80 °C to form a precipitate. The final process is to filter and dry the synthesized precipitate at a temperature of 100 °C to dry.

Preparation of Mg/Al-Biochar

MgAl-LDH was fabricated as in previous research (Badri et al., 2021), through co-precipitation. In order to obtain the composite adding $Mg(NO_3)_2 \cdot 6H_2O$ and $Al(NO_3)_2 \cdot 9H_2O$ were mixed with ratio 3 : 1 and stirred, then as much as 3 g biochar was added and stirred pH 10. The heating process was conducted at 60 °C for 3 days and dried for 24 h.

Adsorption study

The dyes removal was investigated by adsorption times variation, dyes concentration, and temperature variation. The pH effect was studied by setting at pH condition at 2–11. MR and MO, in the amount of 0.02 L 100 mg/L with current pH were added into 0.02 g of the adsorbents and stirred for 2 h under 120 rpm. This process was varied from 5 until 150 minutes. The concentrations of dyes were varied by range 60–100 mg/L and temperatures were conducted at 303–333 K.

Regeneration experiment

A certain amount 0.5 g adsorbent was mixed into 50 mL MO/MR solutions (250 ppm) were shaken for and dried for 2 h. After that, 0.01 g dried adsorbent was placed in 20 mL water and mixed in to HCl (0.01 M). The whole process was conducted for five cycles to study the stability of the materials.

RESULTS AND DISCUSSION

The MgAl-LDH, BC, and MgAl-BC diffraction patterns were displayed in Figure 1 and showed that MgAl-BC has a similar diffractogram compared by the pristine and BC. The basal spacing, which was shown from the diffraction peak of MgAl-BC reached 8.31 Å at 11.81° (003), while the pristine – 7.71Å. According to Lee et al. (2019) the diffraction peak at 16–20° on BC is indicated as silica in the amorphous state. The curve of the adsorption-desorption N_2 on the materials were displayed in Figure 3.

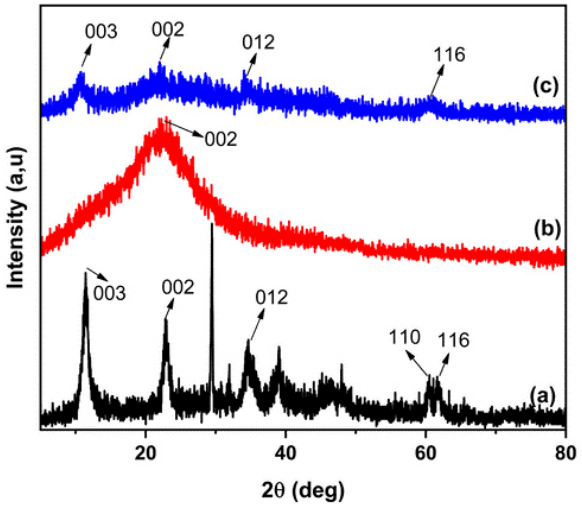

Figure 2. XRD patterns (a) MgAl-LDH (b) BC and (c) MgAl-BC

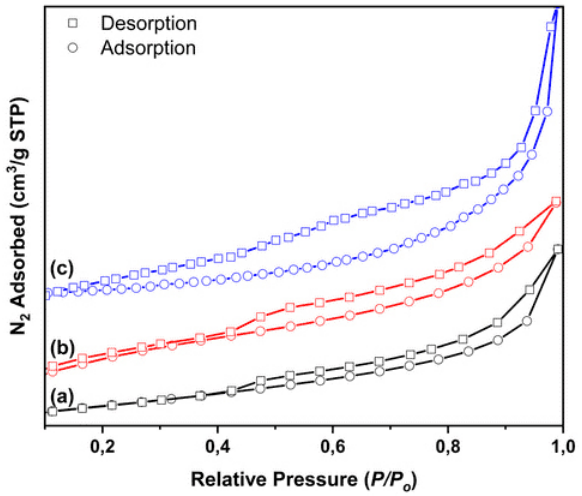

Figure 3. BET of MgAl-LDH (a) BC (b) and MgAl-BC (c)

Table 1. The Surface Area of Adsorbents

Adsorbents	Surface area (m^2/g)	Pore volume (cm^2/g)	Pore size (nm)
MgAl-BC	111.404	10.918	0.062
MgAl-LDH	23.150	36.000	0.092

The curve presented in Figure 2 shows a type IV isotherm pattern with a hysteresis H3. According to IUPAC, the type IV isotherm pattern explains that the material is mesoporous, while the H3 hysteresis pattern indicates that the material has a wide pore distribution (Zhao et al., 2018). Table 1 showed that the surface area of MgAl-BC was higher than MgAl-LDH. On the basis of the above-mentioned phenomenon, the change that occurs from MgAl-LDH to MgAl-BC causes a decrease in agglomeration of LDH, so that the pore size of MgAl-BC is smaller and more regular.

Figure 4 showed the spectra of all the materials. According to (Lee et al., 2019), sharp peak at 1380 cm^{-1} denoted a nitrate ion. A sharp peak around 3400 cm^{-1} showed the -OH stretching existence of water. Figure 4a indicates the presence of nitrate ions at 1381 cm^{-1}.

The vibrational peak of BC (Fig. 4b) at 1620 cm^{-1} ascribed the existence of a C-O bond. The spectrum at 794 cm^{-1} denoted the bonds of Si-O (Yu et al., 2018). The presence of typical peaks of the pristine and the material support in the spectrum of MgAl-BC indicates that the MgAl-BC material is a combination of the two supporting materials.

TG-DTA profile of MgAl-LDH, BC and MgAl-BC were illustrated in Figure 5. The peak in Figure 5a at 105 °C showed the water decomposition of MgAl-LDH surface area and the peak at 380 °C assigned as nitrate decomposition on interlayer. The endothermic peak at 620 °C and 720 °C denoted the decomposition of MgAl-LDH to oxides. The biochar profile in Figure 5b showed the exothermic

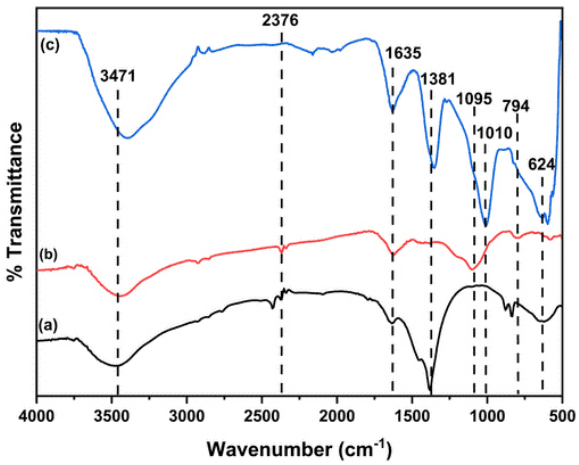

Figure 4. FTIR Spectra of the material MgAl-LDH (a) BC (b) and MgAl-BC (c)

peak at 80 °C which indicated the decomposition of water at biochar surface area. An exothermic peak in Figure 5c at 420 °C of MgAl-BC showed that the composite process required energy to decompose.

Figure 6 illustrated the morphology of the adsorbents. The morphology of MgAl-BC showed the specific character of MgAl-LDH which indicated cubical form and large with shape agglomerated

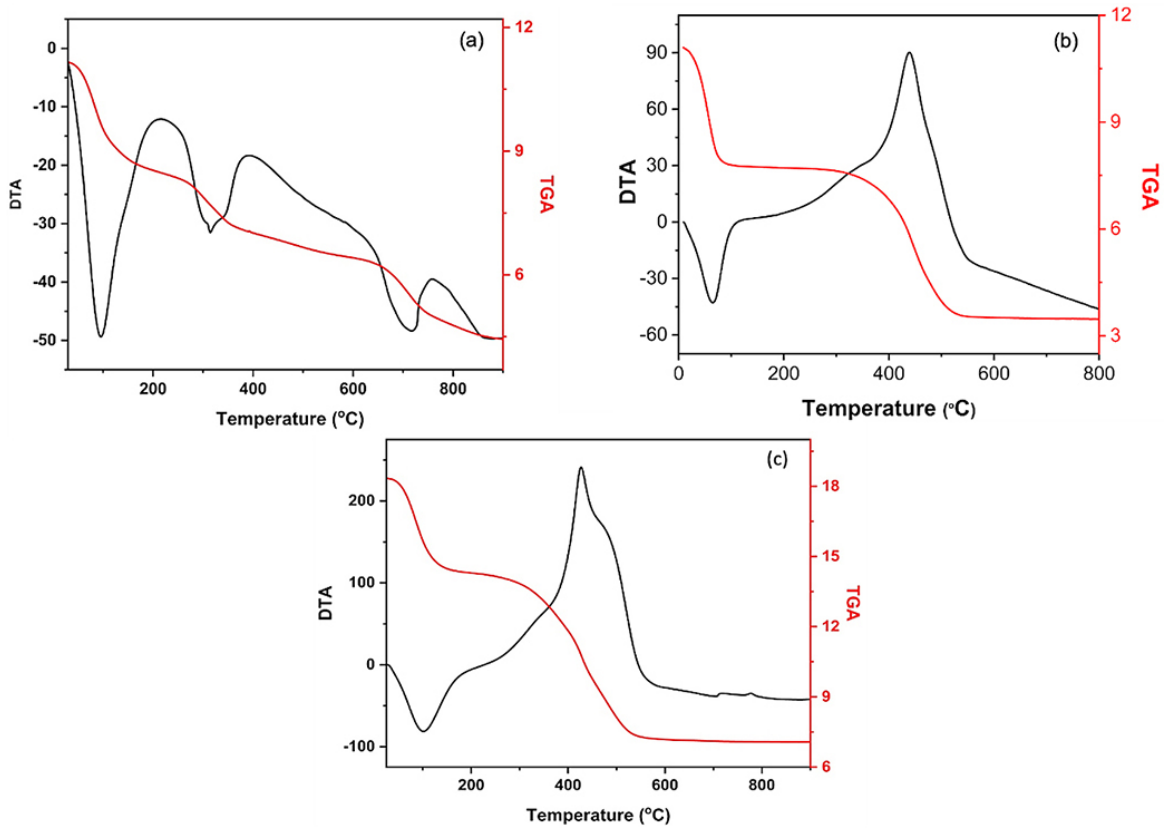

Figure 5.Thermogravimetry patterns of MgAl-LDH (a) BC (b) and MgAl-BC (c)

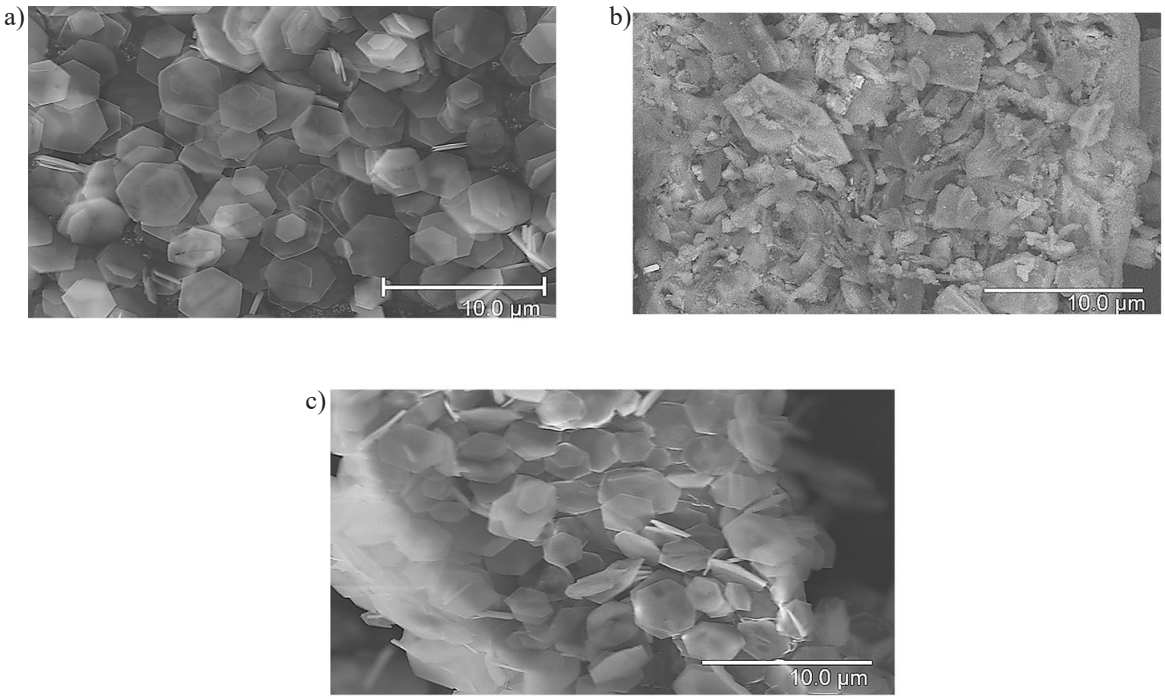

Figure 6. SEM of MgAl-LDH (a) BC (b) and MgAl-BC (c)

particles of biochar. Palapa et al., (2020) assumed the large pore of biochar supported the surface of MgAl-LDH thus, elevating the composite surface area and pores occupation. Meili et al., (2019) assumed that MgAl-BC showed a heterogeneous morphology, which confirmed the formed composite of MgAl-LDH and biochar.

The time variation was carried out to determine the equilibrium state which is presented in Figure 7. On the basis of Figure 7, the equilibrium state of the adsorption process was obtained at 120 minutes. On the other hand, time variation is also used to determine the kinetic parameters which include pseudo-first-order (PFO) and pseudo-second-order (PSO) kinetic models. The results of the determination of the MR and MO adsorption kinetics parameters can be seen in Table 2.

Table 2 shows that the MO adsorption tends to follow the PFO kinetic model, while the MR adsorption tends to follow the PSO kinetic model. Determination of the kinetic model is based on

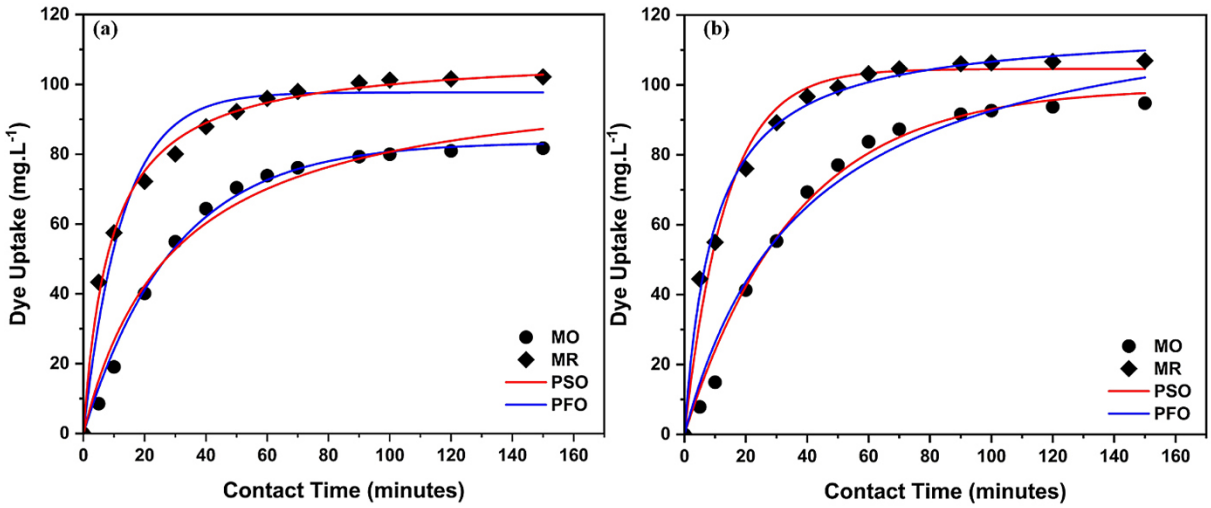

Figure 7. The kinetic parameter of MO (a) MR and (b) onto MgAl-LDH and MgAl-BC (c)

Table 2. The parameters of the PSO and PFO model of Mg/Al-LDH and MgAl-BC

Dye	Adsorbent	Co (mg/L)	Qe (mg/g)	PFO			PSO		
				Qe Calc (mg/g)	R^2	k_1	Qe Calc (mg/g)	R^2	k_2
MO	MgAl-LDH	99.083	81.723	86.726	0.998	0.038	95.237	0.992	0.001
	MgAl-BC		94.810	118.504	0.997	0.395	117.646	0.986	0.001
MR	MgAl-LDH	107.453	102.154	77.757	0.992	0.041	108.694	0.998	0.001
	MgAl-BC		106.930	85.733	0.996	0.051	114.941	0.997	0.001

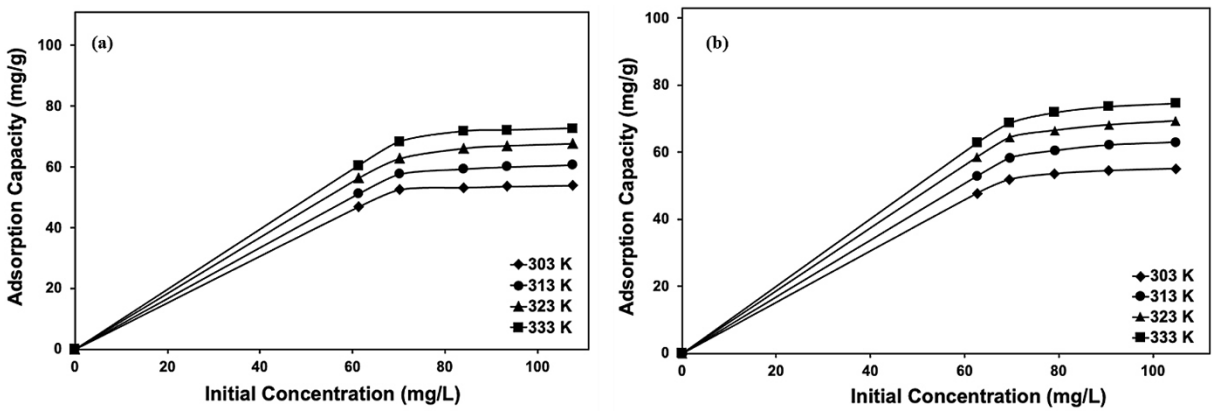

Figure 8. The adsorption of MO on (a) MgAl-LDH and (b) MgAl-BC with concentration and temperature variation

a linear regression value that is closer to 1. The ability of the adsorbent in the adsorption process is supported by the concentration and temperature variation data in Figure 8.

Figures 8 and 9 show that the adsorption process of the MR and MO substances using MgAl-BC has the highest adsorption capacity, this is evidenced by the maximum adsorption capacity data in Table 3 which reaches 107 mg/L. Furthermore, Table 3 also shows the results of determining the isotherm parameters which include the Langmuir and Freundlich adsorption

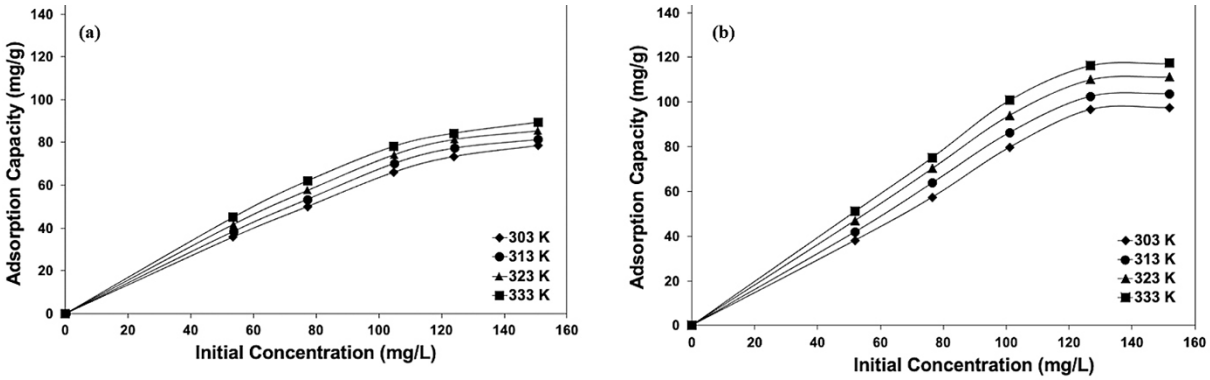

Figure 9. The adsorption of MR on (a) MgAl-LDH and (b) MgAl-BC with concentration and temperature variation

Table 3. Langmuir and Freundlich Model of MO (a) and MR (b) on to MgAl-LDH and MgAl-BC

Dye	Adsorbent	Langmuir model			Feundlich model		
		Qmax	kL	R2	n	kF	R2
MO	MgAl-LDH	74.074	0.178	0.990	3.658	23.115	0.9680
	MgAl-BC	126.582	7.182	0.999	0.566	1.751	0.8986
MR	MgAl-LDH	105.263	0.094	0.998	2.858	22.772	0.9410
	MgAl-BC	142.857	0.022	0.999	0.799	3.211	0.7803

Table 4. MO and MR adsorption capacity comparation using several materials

Adsorbate	Adsorbent	Adsorption Capacity (mg/g)	Reference
MO	Sugar Scum Powder	15.24	(El Maguana et al., 2020)
	Fe2O3–biochar nano-composite (Fe2O3–BC)	20.53	(Chaukura, Murimba, and Gwenzi, 2017)
	Sorel's cement nanoparticles	23.21	(El-Gamal, Amin, and Ahmed, 2015)
	biochar adsorbent (CMC)	39.47	(Yu et al., 2018)
	Fe-Mg LDH	44.843	(Wong, Tay, and Lim, 2020)
	CTS/MMT	70.420	(Umpuch and Sakaew, 2013)
	Multi-walled carbon nanotubes (MWCNTs)	81	(Zhang and Nan, 2015)
	MgAl-LDHs	74.074	This Study
	MgAl-BC	126.582	This Study
MR	Hydroxyapatite	6.675	(Rahmalia, Azis, and Zahrina, 2019)
	biobased microspheres phenylpropenic	17.6	(Yuan et al., 2016)
	White Potato Peel Powder	30.480	(Enenebeaku et al., 2017)
	Palladium nanoparticles on activated carbon	60.970	(Ghaedi et al., 2016)
	Modified chitosan	61.840	(CM Caje et al., 2017)
	Carbon from the Annona Squmosa seed (CAS)	81.970	(Santhi, Manonmani, and Smitha, 2010)
	Activated bio-carbons of raw plants	103	(Bazan-Wozniak and Pietrzak, 2020)
	MgAl-LDHs	105.263	This Study
	MgAl-BC	142.857	This Study

Table 5. Freundlich and Langmuir Isotherm models of MO adsorption on MgAl-LDH and MgAl-BC

T(K)	MgAl-LDH			MgAl/BC		
	ΔH (kJ/mol)	ΔS (kJ/mol)	ΔG (kJ/mol)	ΔH (kJ/mol)	ΔS (J/mol.K)	ΔG (kJ/mol)
303	4.943	0.017	-0.262	6.468	0.021	0.051
313			-0.434			-0.161
323			-0.606			-0.373
333			-0.778			-0.584
303	2.045	0.007	-0.175	5.931	0.020	-0.122
313			-0.248			-0.321
323			-0.322			-0.521
333			-0.395			-0.721
303	1.485	0.005	-0.098	5.520	0.019	-0.221
313			-0.150			-0.411
323			-0.203			-0.600
333			-0.255			-0.790
303	1.239	0.004	-0.015	3.087	0.011	-0.207
313			-0.057			-0.316
323			-0.098			-0.425
333			-0.139			-0.533
303	1.159	0.004	0.062	1.907	0.007	-0.069
313			0.026			-0.134
323			-0.010			-0.199
333			-0.046			-0.265

Table 6. Freundlich and Langmuir Isotherm models of MR adsorption on MgAl-LDH and MgAl-BC

T (K)	MgAl-LDH			MgAl-BC		
	ΔH (kJ/mol)	ΔS (kJ/mol)	ΔG (kJ/mol)	ΔH (kJ/mol)	ΔS (J/mol.K)	ΔG (kJ/mol)
303	26.546	0.093	-1.651	9.111	0.031	-0.339
313			-2.582			-0.651
323			-3.512			-0.963
333			-4.443			-1.275
303	22.105	0.078	-1.446	6.669	0.023	-0.348
313			-2.223			-0.580
323			-3.000			-0.811
333			-3.777			-1.043
303	14.975	0.054	-1.336	4.339	0.016	-0.367
313			-1.874			-0.522
323			-2.412			-0.678
333			-2.950			-0.833
303	10.644	0.038	-0.946	3.613	0.013	-0.386
313			-1.329			-0.518
323			-1.712			-0.650
333			-2.094			-0.782
303	8.173	0.028	-0.184	1.545	0.006	-0.206
313			-0.460			-0.264
323			-0.736			-0.322
333			-1.012			-0.380

isotherm model (Lesbani et al., 2021). The MO and MR dyes adsorption were followed Langmuir. As previously research Palapa et al. (2019) the Langmuir isotherm model indicated of gas systems in monolayer saturation with uniform sites and infinite dilution.

For comparison, there are several adsorbents used for MR and MO adsorption which are presented in Table 4. These data showed in this research the adsorption capacity of the adsorbents had higher results than the other. Thus, it concluded that the materials were good adsorbents to remove MO and MR.

Tables 5 and 6 displayed the thermodynamic data from the MO and MR adsorption processes. The adsorption using MgAl-BC and the pristine generated Gibbs energy with negative values which showed spontaneous condition (Normah et al., 2021). The positive enthalpy showed endothermic adsorption (Lesbani et al., 2021) and entropy energy (ΔS°) with signified the increasing of the randomness (Zhao et al., 2018).

The ability of the adsorbent in the adsorption process is also proven by the adsorption selectivity process carried out with time variations. The results of the adsorption selectivity are shown through the UV-Vis spectrum of the mixture of MO and MR in Figure 10. There was a decrease in absorbance at the MO peak compared to MR, which confirmed that the MgAl-LDH, BC, and MgAl-BC adsorbents were easier in the MO adsorption process.

The ability of the adsorbent in the regeneration process in Figure 11 confirms that MgAl-BC, as a composite material, has better structural stability than MgAl-LDH. MgAl-BC is able to go through the regeneration process up to 5 cycles, while MgAl-LDH only lasts up to the 4th cycle. the use of hydrochloric acid as a solvent during the desorption process made it possible that the MgAl-LDH layer was exfoliated due to the use of acid.

CONCLUSIONS

MgAl-BC has been successfully developed as a material that has the potential to overcome dye contamination such as MR and MO. The

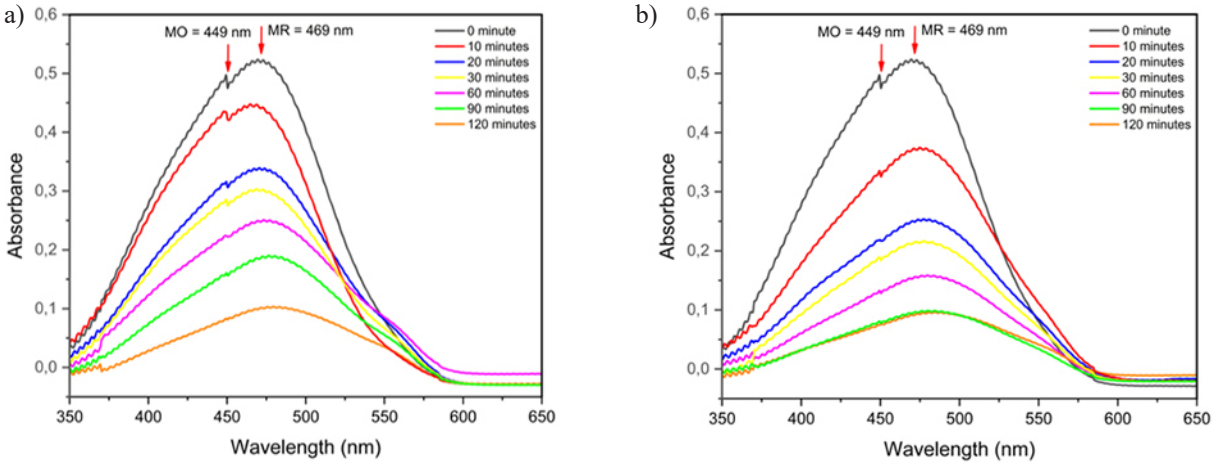

Figure 10. Adsorption Selectivity of MR and MO by using MgAl-LDH (a) and MgAl-BC (b)

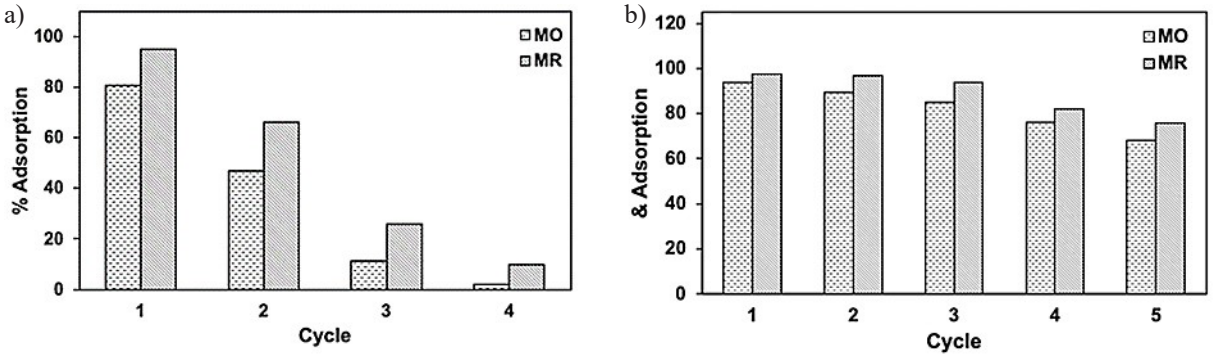

Figure 11. The Regeneration of MO and MR on MgAl-LDH (a) and MgAl-BC (b)

ability of MgAl-BC in overcoming MR and MO is evidenced by the adsorption capacity data which reached 128,205 mg/g for MO and 142,857 mg/g for MR. The adsorbent regeneration process has also proven that MgAl-BC has a more stable structure than MgAl-LDH, this is shown from the regeneration data of MgAl-BC which lasts up to 5 cycles.

Acknowledgments

The authors thank DIPA of Public Service Agency of Sriwijaya University 2021. SP DIPA-023.17.2.677515/2021 on November 23, 2020. In accordance with the Rector's Decree Number: 0014/UN9/SK.LP2M.PT/2021, on May 25, 2021. This article is additional output research of Hibah Profesi 2021. Special thanks for the Research Center of Inorganic Materials and Complexes of the Faculty of Mathematics and Natural Sciences, Sriwijaya University for analysis and instruments.

REFERENCES

1. Ayawei N., Angaye S.S., Wankasi D., Dikio E.D. 2015. Synthesis, Characterization and Application of Mg/Al Layered Double Hydroxide for the Degradation of Congo Red in Aqueous Solution. Open Journal of Physical Chemistry, 5(3), 56–70.
2. Badri A.F., Siregar P.M.S.B.N., Palapa N.R., Mohadi R., Mardiyanto M., Lesbani A. 2021. Mg-Al/Biochar Composite with Stable Structure for Malachite Green Adsorption from Aqueous Solutions. Bulletin of Chemical Reaction Engineering & Catalysis, 16(1), 149–160.
3. Bharali D., Deka R.C. 2017. Adsorptive removal of congo red from aqueous solution by sonochemically synthesized NiAl layered double hydroxide. Journal of Environmental Chemical Engineering, 5(2), 2056–2067.
4. Cantarella M., Sanz R., Buccheri M.A., Ruffino F., Rappazzo G., Scalese S., Impellizzeri G., Romano L., Privitera V. 2016. Immobilization of nanomaterials in PMMA composites for photocatalytic removal of dyes, phenols and bacteria from water. Journal of Photochemistry and Photobiology A: Chemistry, 321, 1–11.
5. Demissie H., An G., Jiao R., Ritigala T., Lu S., Wang D. 2021. Modification of high content nanocluster-based coagulation for rapid removal of dye from water and the mechanism. Separation and Purification Technology, 259, 117845.
6. Duan C., Meng X., Liu C., Lu W., Liu J., Dai L., Wang W., Zhao W., Xiong C., Ni Y. 2019. Carbohydrates-rich corncobs supported metal-organic frameworks as versatile biosorbents for dye removal and microbial inactivation. Carbohydrate Polymers, 222, 115042.
7. Gholami P., Dinpazhoh L., Khataee A., Hassani A., Bhatnagar A. 2020. Facile hydrothermal synthesis of novel Fe-Cu layered double hydroxide/biochar nanocomposite with enhanced sonocatalytic activity for degradation of cefazolin sodium. Journal of Hazardous Materials, 381(5), 120742.
8. Juleanti N., Palapa N.R., Taher T., Hidayati N., Putri B.I., Lesbani A. 2021. The Capability of Biochar-Based CaAl and MgAl Composite Materials as Adsorbent for Removal Cr (VI) in Aqueous Solution. Science and Technology Indonesia, 6(3), 156–165.
9. Lee S.Y., Choi J.W., Song K.G., Choi K., Lee Y.J., Jung K.W. 2019. Adsorption and mechanistic study for phosphate removal by rice husk-derived biochar functionalized with Mg/Al-calcined layered double hydroxides via co-pyrolysis. Composites Part B: Engineering, 176, 107209.
10. Lesbani A., Azmi M.F., Palapa N.R., Taher T., Andreas R., Mohadi R. 2021. Ni/Cr- [α -$SiW_{12}O_{40}$] Layered Double Hydroxide as Effective Adsorbent of Iron (II) From Aqueous Solution. Eurasian Chemistry Technology Journal, 23(2021), 103–110.
11. Lesbani A., Palapa N.R., Sayeri R.J., Taher T., Hidayati N. 2021. High Reusability of NiAl LDH/Biochar Composite in the Removal Methylene Blue from Aqueous Solution. Indonesian Journal of Chemistry, 21(2), 421–434.
12. Lu Y., Jiang B., Fang L., Ling F., Gao J., Wu F., Zhang X. 2016. High performance NiFe layered double hydroxide for methyl orange dye and Cr(VI) adsorption. Chemosphere, 152, 415–422.
13. Meili L., Lins P.V., Zanta C.L.P.S., Soletti J.I., Ribeiro L.M.O., Dornelas C.B., Silva T.L., Vieira M.G.A. 2019. MgAl-LDH/Biochar composites for methylene blue removal by adsorption. Applied Clay Science, 168, 11–20.
14. Natarajan S., Anitha V., Gajula G.P., Thiagarajan V. 2020. Synthesis and Characterization of Magnetic Superadsorbent Fe_3O_4-PEG-Mg-Al-LDH Nanocomposites for Ultrahigh Removal of Organic Dyes. ACS Omega, 5(7), 3181–3193.
15. Normah N., Juleanti N., Siregar P.M.S.B.N., Wijaya A., Palapa N.R., Taher T., Lesbani A. 2021. Size Selectivity of Anionic and Cationic Dyes Using LDH Modified Adsorbent with Low-Cost Rambutan Peel to Hydrochar. Bulletin of Chemical Reaction Engineering & Catalysis, 16(4), 869–880.
16. Oktriyanti M., Palapa N.R., Mohadi R., Lesbani A. 2019. Indonesian Journal of Environmental Management and Sustainability Modification Of Zn-Cr Layered Double Hydroxide With Keggin Ion. Indonesian Journal of Environmental Management and Sustainability, 3(3), 93–99.

17. Palapa N.R., Mohadi R., Rachmat A., Lesbani A. 2020. Adsorption Study of Malachite Green Removal from Aqueous Solution Using Cu/M^{3+} (M^{3+}=Al,Cr) Layered Double Hydroxide. Mediterranean Journal of Chemistry, 10(1), 33–45.
18. Palapa N.R., Saria Y., Taher T., Mohadi R., Lesbani A. 2019. Synthesis and Characterization of Zn/Al, Zn/Fe, and Zn/Cr Layered Double Hydroxides: Effect of M^{3+} ions Toward Layer Formation. Science and Technology Indonesia, 4(2), 36–39.
19. Puchana-Rosero M.J., Adebayo M.A., Lima E.C., Machado F.M., Thue P.S., Vaghetti J.C.P., Umpierres C.S., Gutterres M. 2016. Microwave-assisted activated carbon obtained from the sludge of tannery-treatment effluent plant for removal of leather dyes. Colloids and Surfaces A: Physicochemical and Engineering Aspects, 504, 105–115.
20. Santos R.M.M. dos Gonçalves R.G.L., Constantino V.R.L., Santilli C.V., Borges P.D., Tronto J., Pinto F.G. 2017. Adsorption of Acid Yellow 42 dye on calcined layered double hydroxide: Effect of time, concentration, pH and temperature. Applied Clay Science, 140, 132–139.
21. Streit A.F.M., Côrtes L.N., Druzian S.P., Godinho M., Collazzo G.C., Perondi D., Dotto G.L. 2019. Development of high quality activated carbon from biological sludge and its application for dyes removal from aqueous solutions. Science of the Total Environment, 660, 277–287.
22. Tran H.N., Lin C.C., Chao H.P. 2018. Amino acids-intercalated Mg/Al layered double hydroxides as dual-electronic adsorbent for effective removal of cationic and oxyanionic metal ions. Separation and Purification Technology, 192, 36–45.
23. Vinsiah R., Mohadi R., Lesbani A. 2020. Indonesian Journal of Environmental Management and Sustainability Performance of Graphite for Congo Red and Direct Orange Adsorption. Indonesian Journal of Environmental Management and Sustainability, 4(4), 125–132.
24. Wijaya A., Siregar P.N.B.S.M., Priambodo A., Palapa N.R., Taher T., Lesbani A. 2021. Innovative Modified of Cu-Al/C(C=Biochar, Graphite) Composites for Removal of Procion Red from Aqueous Solution. Science and Technology Indonesia, 6(4), 228–234.
25. Yu J., Zhang X., Wang D., Li P. 2018. Adsorption of methyl orange dye onto biochar adsorbent prepared from chicken manure. Water Science and Technology, 77(5–6), 1303–1312.
26. Zhao G., Liu L., Li C., Zhang T., Yan T., Yu J., Jiang X., Jiao F. 2018. Construction of diatomite/ZnFe layered double hydroxides hybrid composites for enhanced photocatalytic degradation of organic pollutants. Journal of Photochemistry and Photobiology A: Chemistry, 367, 302–311.